

See discussions, stats, and author profiles for this publication at: <https://www.researchgate.net/publication/46484866>

# Physical Consistency of Generalized Linear Driving Force Models for Adsorption in a Particle

ARTICLE *in* INDUSTRIAL & ENGINEERING CHEMISTRY RESEARCH · AUGUST 2005

Impact Factor: 2.59 · DOI: 10.1021/ie050329z · Source: OAI

---

CITATIONS

6

---

READS

35

4 AUTHORS, INCLUDING:



**G. Fernandez-Anaya**

Universidad Iberoamericana Ciudad de México

**131** PUBLICATIONS **398** CITATIONS

SEE PROFILE



**Francisco J. Valdes-Parada**

Metropolitan Autonomous University

**103** PUBLICATIONS **606** CITATIONS

SEE PROFILE



**J. Alberto Ochoa-Tapia**

Metropolitan Autonomous University

**82** PUBLICATIONS **1,758** CITATIONS

SEE PROFILE

# Physical Consistency of Generalized Linear Driving Force Models for Adsorption in a Particle

José Álvarez-Ramírez,\* Guillermo Fernández-Anaya,<sup>†</sup>  
Francisco J. Valdés-Parada, and J. Alberto Ochoa-Tapia

Departamento de Ingeniería de Procesos e Hidráulica, Universidad Autónoma Metropolitana-Iztapalapa,  
Apartado Postal 55-534, Mexico, D.F., P.C. 09340 Mexico

The so-called (first-order) linear driving force (LDF) model for gas adsorption kinetics is frequently and successfully used for analysis and design of adsorptive processes because it is simple, analytical, and physically consistent. Yet, for certain operating conditions, such as cyclic adsorption and desorption, significant differences between the LDF model and the rigorous Fickian diffusion (FD) model can be found. In principle, increasing the order of the approximate LDF model can yield predictions closer to the FD model. As in the classical first-order LDF model, generalized LDF must be consistent with the physics of the FD model. This paper provides a minimal set of properties that generalized LDF models should meet in order to be physically consistent. This is done by showing that the FD model describes positive real dynamics, which are closely related to the thermodynamics of the adsorption–diffusion process. In this form, a generalized LDF model should inherit this property in order to guarantee that the main thermodynamic characteristics of the adsorption–diffusion dynamics will be retained to some extent.

## 1. Introduction

Consider diffusion and adsorption dynamics in a uniformly porous spherical particle. The mass balance equation describing the concentration profile  $c(r_p, t)$  inside the particle is

$$\epsilon_p \frac{\partial c}{\partial t} = D_p \frac{1}{r^2} \frac{\partial}{\partial r} \left( r^2 \frac{\partial c}{\partial r} \right) - K \frac{\partial c}{\partial t}$$

where  $r$  is the radial particle coordinate,  $\epsilon_p$  is the porosity in the particle, and  $D_p$  is the effective pore diffusivity based on the total area. A linear adsorption equilibrium on the pore walls with equilibrium constant  $K$  was assumed. Equivalently, the above equation can be written in dimensionless form as

$$\frac{(\epsilon_p + K)R_p^2}{D_p} \frac{\partial q}{\partial t} = \frac{1}{\xi^2} \frac{\partial}{\partial \xi} \left( \xi^2 \frac{\partial q}{\partial \xi} \right)$$

where  $q = (\epsilon_p + K)c/c^*$  is a dimensionless concentration per unit volume in the particle,  $c^*$  is a characteristic concentration, and  $\xi = r/R_p$  is the dimensionless radial variable. A diffusion time constant can be defined as

$$\tau_D = \frac{(\epsilon_p + K)R_p^2}{D_p}$$

By introducing the dimensionless time variable  $\tau = t/\tau_D$ ,

\* To whom correspondence should be addressed. División de Ciencias Básicas e Ingeniería, Universidad Autónoma Metropolitana-Iztapalapa, Apartado Postal 55-534, 09340, Mexico. Tel.: +52-55-57244648. Fax: +52-55-58044900. E-mail: jjar@xanum.uam.mx. Also at Programa de Investigación en Matemáticas Aplicadas y Computación, Instituto Mexicano del Petróleo.

<sup>†</sup> Departamento de Matemáticas, Universidad Iberoamericana.

one obtains the standard formulation referred to as the pore diffusion model:

$$\frac{\partial q}{\partial \tau} = \frac{1}{\xi^2} \frac{\partial}{\partial \xi} \left( \xi^2 \frac{\partial q}{\partial \xi} \right) \quad (1)$$

The boundary conditions, for all  $\tau \geq 0$ , are

$$\begin{aligned} \text{at } \xi = 0, \quad \frac{\partial q}{\partial \xi} &= 0 \\ \text{at } \xi = 1, \quad q &= f(\tau) \end{aligned} \quad (2)$$

and the initial condition, for all  $\xi \in [0, 1]$ , is often taken as

$$\text{at } \tau = 0, \quad q = 0 \quad (3)$$

Equations 1–3 will be referred to as the Fickian diffusion (FD) model. Sometimes, for different values of the “design parameter”  $f(\tau)$ , repeated solutions of eqs 1–3 have to be obtained for optimization-based designs or simply for simulation purposes. An important example is the cyclic operation of adsorption systems where the solution of the diffusion model must be repeated over many cycles of operation in order to establish the final cyclic steady-state separation performance of the overall process.<sup>1</sup> Although the solution of the problem (eqs 1–3) can be carried out with either analytical or numerical methods, it is coupled with the simultaneous solution of mass, heat, and momentum balance equations at the particle and column scales. As a result, the model of the separation equipment may require impractically large computation times for process simulation under realistic conditions. Spouted bed particle drying is another interesting example where repeated solution of a model similar to eqs 1–3 must be repeated in every integration step.<sup>2</sup> The computational burden involved in the numerical solution can be

drastically increased when the particles display a wide size distribution. In this case, the diffusion model must be solved for each particle distribution fraction. Given the complexity of the solution of the diffusion model when coupled with heat, mass, and momentum balance equations at separation-equipment scales, there is an incentive to obtain finite-dimensional (i.e., low-order) models to accurately describe the diffusion phenomena into porous particles. In principle, mathematically simple, e.g., ordinary differential equations, diffusion models can significantly reduce the computational times required for realistic process simulations. Finite-dimensional models are also of great importance for the design of model-based controllers for adsorption–diffusion processes. In fact, reduced-order models that retain the main dynamic characteristics of the process can be used to design practical controllers to regulate the operation of adsorption processes.

Let

$$\langle q \rangle(\tau) \equiv 3 \int_0^1 q(\xi, \tau) \xi^2 d\xi \quad (4)$$

be the average particle concentration. The derivation of simple models for adsorption–diffusion dynamics was studied by Glueckauf and Cotes,<sup>3</sup> who proposed the following (first-order) linear driving-force (LDF) model structure:

$$\frac{d\langle q \rangle}{d\tau} = k(f(\tau) - \langle q \rangle), \quad k > 0 \quad (5)$$

The approximate model (eq 5) is consistent with the physical structure of the adsorption–diffusion process, since it establishes that the amount entering or leaving the particles is proportional to the difference between the existing average particle concentration  $\langle q \rangle(\tau)$  and that obtained at surface conditions  $f(\tau)$ . The attractiveness of the model (eq 5) relies in its simplicity; indeed, it is a first-order ordinary linear differential equation with an analytical solution. Glueckauf<sup>4</sup> recommended the *empirical* value  $k = 14$ . In a subsequent work, Glueckauf<sup>5</sup> obtained the slightly bigger value  $k = 15$ , which was obtained from the exact analytical solution  $\langle q \rangle(\tau)$  and considered only the first-order expansion terms. Interestingly, Liaw et al.<sup>6</sup> have showed that the value  $k = 15$  can be derived by assuming a quadratic approximation to the concentration profile  $q(\xi, \tau)$ . Departing from Glueckauf's work, LDF models have been the standard approach for fast simulation and design of a wide variety of adsorption/desorption processes (see ref 1 and references therein).

LDF models have been successfully used for the analysis and design of adsorptive processes because of their simplicity, analytical solution, and physical consistency. Yet, for certain operating conditions, such as cyclic adsorption and desorption, significant differences between the LDF model and the rigorous Fickian diffusion (FD) model can be displayed.<sup>7</sup> As pointed out by Lee and Kim,<sup>8</sup> first-order LDF models are suitable for elucidating the essential features of adsorption–diffusion processes but may be too rough for detailed analysis and optimization. In principle, increasing the order of the approximant can lead to better predictions of the process dynamics.<sup>8</sup> High-order models can be proposed as follows. The solution of eqs 1–3 in the

Laplace domain can be expressed as

$$\begin{aligned} \langle Q \rangle(s) &= 3 \left( \frac{\coth \sqrt{s}}{\sqrt{s}} - \frac{1}{s} \right) F(s) \\ &\equiv G(s)F(s) \end{aligned} \quad (6)$$

where  $s$  is the Laplace variable,  $\langle Q \rangle(s)$  and  $F(s)$  are, respectively, the Laplace transform of  $\langle q \rangle(\tau)$  and  $f(\tau)$ , and  $G(s)$  is the transfer function relating  $\langle Q \rangle(s)$  and  $F(s)$  (i.e.,  $F(s) \xrightarrow{G(s)} \langle Q \rangle(s)$ ). One has that, for an arbitrary function  $f(\tau)$ , the approximation of the adsorption–diffusion dynamics described by eqs 1–3 is equivalent to the approximation of the transfer function  $G(s)$ . In this way, the transfer function

$$H_1(s) = \frac{1}{\frac{s}{k} + 1} \quad (7)$$

is a first-order approximation to the FD transfer function  $G(s)$  and corresponds to the Laplace transform of the classical LDF model (eq 5). High-order approximations can be proposed as rational finite-dimensional functions as follows:

$$H_n^m(s) = \frac{B_n(s)}{A_n(s)} = \frac{b_m s^m + b_{m-1} s^{m-1} + \dots + b_1 s + b_0}{a_n s^n + a_{n-1} s^{n-1} + \dots + a_1 s + a_0}, \quad m \geq 0, \quad n \geq 1, \quad m \leq n \quad (8)$$

In this way, the classical LDF model (eq 5) corresponds to  $m = 0$  and  $n = 1$ . It should be stressed that the condition  $m \leq n$  is imposed to guarantee the causality of the dynamics induced by  $H_n^m(s)$  (see ref 9). Different methods can be designated to determine the value of the parameters  $\{a_n, \dots, a_0; b_m, \dots, b_0\}$ . For instance, an approximate model matching  $H_n^m(s) \approx G(s)$  around steady-state conditions  $s \rightarrow 0^+$  via Taylor expansion can be used. It is expected that, in general, the value of the coefficients could depend on the underlying approximation procedure.<sup>8</sup>

It has been mentioned above that the classical LDF model (eq 5, represented as  $H_1^0(s)$ ) is physically consistent with the FD model  $G(s)$ . Although a precise physical consistence definition for the approximation problem  $H_1^0(s) \approx G(s)$  is not given in the literature,<sup>8</sup> physical consistence refers to the facts that the time-domain model is asymptotically stable and the amount of mass entering or leaving the particles is proportional to the difference between the existing average concentration  $\langle q \rangle(\tau)$  and that obtained at the surface conditions  $f(\tau)$ . In this form, as in the classical first-order LDF model  $H_1^0(s)$ , high-order approximants  $H_n^m(s)$  should be consistent with the physics of the FD model. Lee and Kim<sup>8</sup> heuristically showed that only approximants with either  $m = n - 1$  or  $m = n$  yield physically consistent finite-dimensional models in the sense that these are stable. In fact, approximants with  $m < n - 1$  yield unstable finite-dimensional models, which are not consistent with the physics of the adsorption–diffusion process.

The aim of this paper is 2-fold:

- To propose the passivity property of the transfer functions as a framework to evaluate the physical consistency of the approximation problem  $H_n^m(s) \approx G(s)$ . This is done by showing that the FD model  $G(s)$  describes *positive real* (PR) dynamics.<sup>10</sup>

• To use such a framework to back up the heuristic observation made by Lee and Kim<sup>8</sup> that only approximations with either  $m = n - 1$  or  $m = n$  yield physically consistent finite-dimensional models.

Although algebraic in nature, the importance of the PR concept relies on the fact that it can be linked to the thermodynamics of the adsorption–diffusion process.<sup>11</sup> Hence, a generalized LDF model  $H_n^m(s)$  should inherit the PR property to guarantee that the approximate dynamics are consistent with the thermodynamics of the rigorous Fickian diffusion model. In this form, our results show that physically consistent LDF models must meet the constraints that  $m = n - 1$  and the polynomials  $A_n(s)$  and  $B_m(s)$  are critically stable (i.e., all the roots have a negative or zero real part).

## 2. Passivity Property of the FD Model $G(s)$

In this section, some structural properties of the FD model  $G(s)$  will be studied. In particular, it will be shown that  $G(s)$  is a PR function. The definition of a PR functions is derived from electrical network theory. In ref 10, the following definition has been given for PR transfer functions by an appeal of network theory: “A function  $G(s)$  of complex variable  $s = \sigma + j\omega$  is PR if: (i)  $G(s)$  is real for  $s$  real, (ii)  $G(s)$  is analytic in  $\text{Re}[s] > 0$ , and (iii)  $\text{Re}[G(s)] > 0$  for all  $\text{Re}[s] \geq 0$ ”.

Condition (ii) states that the transfer function  $G(s)$  does not have unstable poles (i.e., poles with a positive real part). On the other hand, condition (iii) corresponds to the fact that a PR dynamic system does not generate energy. The importance of PR functions relies on the fact that their physical interpretation as a PR transfer function can be realized as a driving point impedance of a passive electrical network. In addition, a passive network is one that does not generate energy, i.e., a network consisting only of resistors and capacitors.

Positive realness as described above is an algebraic condition to establish the passivity of a linear process system. In turn, the passivity property of a process system is closely linked to irreversible thermodynamics concepts. A nice interpretation of passivity via the Clausius–Planck inequality was given in an elegant paper by Ydstie and Alonso,<sup>11</sup> who showed how passivity and irreversible thermodynamics can be related for macroscopic systems. Specifically, they showed that a process system can be described by inventory dynamics, which is the case of the adsorption–diffusion process described by eqs 1–3, as long as the existence of a positive storage function can be demonstrated. As a matter of fact, the PR definition as given above implies the existence of such a storage function via the so-called Kalman–Yakubovich–Popov Lemma.<sup>10</sup> It should be mentioned that these functions are a particular case of the so-called dissipative functions.<sup>10</sup> In this paper, rather than showing the existence of a positive storage function for the process system (eqs 1–3), we exploit the linearity of the system to demonstrate the PR by means of a direct application of the definition given above.

The following properties of the FD model  $G(s)$  can be established:

• **Property 1.**  $\lim_{s \rightarrow 0} G(s) = 1$ . This property says that the FD model  $G(s)$  has unitary steady-state gain. In other words, if the surface concentration  $f(\tau)$  is a constant, say  $f^*$ , then the steady-state average concentration value  $\langle q \rangle = f^*$ .

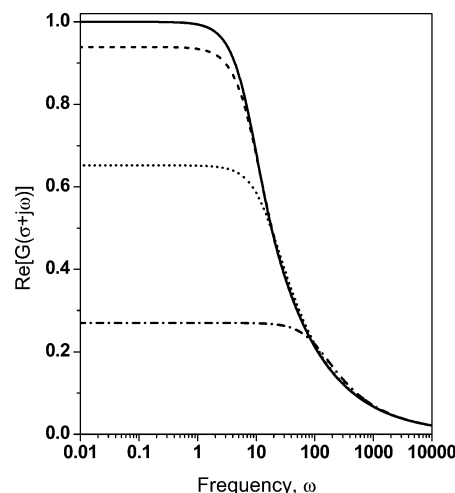


**Figure 1.** Real part of the complex function  $G(\sigma + j\omega)$  for different values of  $\sigma \geq 0$ . It is noticed that  $\text{Re}[G(\sigma + j\omega)] > 0$  for all  $\omega \in \mathbb{R}$  along four decades: —  $\sigma = 0$ ; - - -  $\sigma = 1$ ; ...  $\sigma = 10$ ; - · - ·  $\sigma = 100$ .

• **Property 2.**  $\lim_{s \rightarrow \infty} G(s) = 0$ . This implies that the modulus  $|G(j\omega)|$  rolls down to zero as  $\omega \rightarrow \infty$ . High-frequency components of the forcing function  $f(\tau)$  are washed out by  $G(j\omega)$ , so that their effects on the average concentration dynamics  $\langle q \rangle(\tau)$  can be neglected.

• **Property 3.** The FD transfer function  $G(s) = 3((\coth \sqrt{s})/\sqrt{s} - 1/s)$  is a PR function. To demonstrate this property, we follow the PR function definition given above. It is clear that  $G(s)$  satisfies item (i), since  $G(s)$  is real for  $s$  real. Let us prove item (ii). To this end, observe that

$$\frac{\coth \sqrt{s}}{\sqrt{s}} - \frac{1}{s} = \frac{s \cosh \sqrt{s} - \sqrt{s} \sinh \sqrt{s}}{(\sqrt{s})^3 \sinh \sqrt{s}}$$

It is apparent that  $s = 0$  is a pole of  $G(s)$ . However, because  $\lim_{s \rightarrow 0} 3[(\coth \sqrt{s})/\sqrt{s} - 1/s] = 1$ ,  $s = 0$  is not actually a pole of  $G(s)$ . In this way, the poles of  $G(s)$  correspond to the zeros of the function  $\sinh \sqrt{s}$ . Notice that

$$\sinh \sqrt{s} = 0 \Rightarrow e^{\sqrt{s}} - e^{-\sqrt{s}} = 0 \Rightarrow e^{\sqrt{s}}(1 - e^{-2\sqrt{s}}) = 0$$

where  $|e^{\sqrt{s}}| \geq 1$  for  $\text{Re}[s] > 0$ . Therefore,

$$e^{\sqrt{s}}(1 - e^{-2\sqrt{s}}) = 0 \Rightarrow e^{-2\sqrt{s}} = 1$$

As  $\sqrt{s} = jk\pi$ ,  $k \in \{0, \pm 1, \pm 2, \dots\}$ , the zeros of  $\sinh \sqrt{s}$  are to be located at  $s_k = (jk\pi)^2 = -k^2\pi^2 < 0$  for  $k \in \{0, \pm 1, \pm 2, \dots\}$ . As a matter of fact, these poles correspond to the eigenvalues of the spatial operator  $\partial^2/\partial \xi^2$ , which allows a Fourier expansion of the time-domain solution as  $\sim \sum_{k=1}^{\infty} \exp(-k^2\pi^2\tau)$  (see, for instance, ref 12). As  $s_k = -k^2\pi^2 < 0$ , one has it that  $G(s)$  has no poles in  $\text{Re}[s] > 0$ . Further, since  $-k^2\pi^2 < 0$ , the transfer function  $G(s)$  is asymptotically stable. That is, for  $f(\tau) = f^*$ , one has that  $\langle q \rangle(\tau) \rightarrow f^*$  as  $\tau \rightarrow \infty$ . The proof of item (iii) involves tedious but straightforward algebraic manipulations. The interested reader is referred to the appendix. Here, we provide numerical evidences by computing  $\text{Re}[G(\sigma + j\omega)]$  for  $\sigma \geq 0$ . Figure 1 shows the real part of the complex function  $G(\sigma + j\omega)$  for different values of  $\sigma \geq 0$ . It is noticed that  $\text{Re}[G(\sigma + j\omega)] > 0$  for all  $\omega \in \mathbb{R}$  along four decades. As implied by Property 2,  $\text{Re}[G(\sigma + j\omega)]$



approaches zero from above only as  $\omega \rightarrow \infty$ . This shows that, in fact,  $G(s)$  is a PR function.

In this form, Properties 1–3 lead to the observation that the transfer function  $G(s)$  has the structure of a *passive low-pass filter*.

### 3. Inherited Structure of Approximate Models

$H_n^m(s)$

As shown in the above section, the FD model  $G(s)$  has an infinite number of poles located at  $s_k = -k^2\pi^2$  for  $k \in \{0, \pm 1, \pm 2, \dots\}$ . This means that  $G(s)$  corresponds to an infinite-dimensional dynamic system. Approximate finite-dimensional modes are given as rational functions  $H_n^m(s)$  (see eq 8). A minimal approximation requirement is that rational models  $H_n^m(s)$  should satisfy Properties 1–3 discussed above. This is done as follows:

- From eq 8, it is easy to see that  $\lim_{s \rightarrow 0} H_n^m(s) = b_0/a_0$ . In this way, the constraint  $a_0 = b_0$  must be satisfied. In particular, without loss of generality, one can choose  $a_0 = b_0 = 1$ .

- To satisfy Property 2, it is clear that the constraint  $m < n$  must be met. Otherwise,  $m = n$  implies that  $\lim_{s \rightarrow \infty} H_n^m(s) = b_m/a_n$  which is different from zero unless  $b_m = 0$  or  $m < n$ .

- To find the constraints on the structure of  $H_n^m(s)$  induced by Property 3, let us recall the following PR concept for rational functions:<sup>10</sup> If a rational function of the form given by eq 8 is PR, then all the coefficients  $\{a_n, \dots, a_0, b_m, \dots, b_0\}$  are positive and  $|n - m| \leq 1$ . The later inequality implies that either  $n - m = -1$ ,  $n = m$ , or  $m = n - 1$ . Causality arguments forbid the inequality  $n - m = -1$ . On the other hand, the constraint  $m < n$  established in the above paragraph forbids the equality  $m = n$ . Consequently, the numerator and denominator polynomial powers are constrained to satisfy  $m = n - 1$ .

The framework based on the PR concept allowed us to define a class of rational function approximants that are physically consistent with the rigorous FD model. Since the PR concept is closely linked to passivity, which is linked with irreversible thermodynamics via mass inventory,<sup>11</sup> PR approximants  $H_n^{n-1}(s)$  with  $\lim_{s \rightarrow 0} H_n^m(s) = 1$  and  $\lim_{s \rightarrow \infty} H_n^m(s) = 0$  retain, to some extent, the thermodynamic properties of the FD model  $G(s)$ . In this form, the framework used above is suitable to obtain finite-dimensional descriptions of adsorption–diffusion process dynamics.

### 4. Discussion

The results obtained in the above section have interesting practical implications. Some of them are related to the structure of the approximant class, and others are related to the application of such approximation functions to general dynamic conditions.

(a) Lee and Kim<sup>8</sup> observed that approximants with  $m = n$  or  $m = n - 1$  meet the criterion of being stable models, although no justification for this observation was given. Our analysis shows that approximants with  $m = n$  do not meet the criterion  $\lim_{s \rightarrow \infty} H_n^m(s) = 0$ . On the other hand, our results show that only approximants with  $m = n - 1$  (i.e.,  $H_n^{n-1}(s)$ ) inherit Properties 1–3 of the rigorous FD model  $G(s)$ , so that approximants with  $m = n$  are discarded. Indeed, our results provide a backup to the empirical observations made by Lee and Kim.<sup>8</sup>

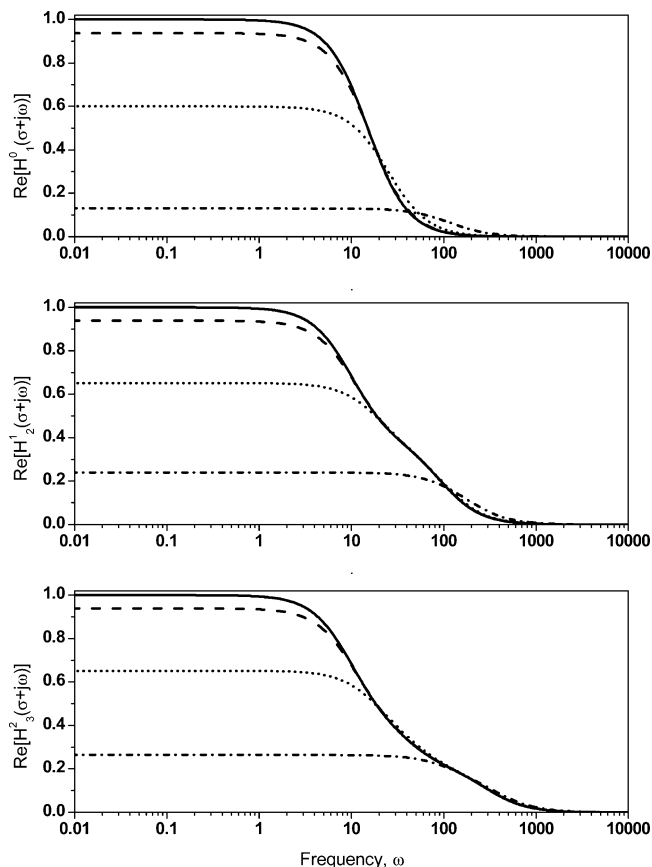


**Figure 2.** Real part of the approximants where it is observed that  $\text{Re}[H_n^{n-1}(\sigma + j\omega)] > 0$  for all  $\omega \in \mathbb{R}$  along four decades: —  $\sigma = 0$ ; ---  $\sigma = 1$ ; ...  $\sigma = 10$ ; - · - ·  $\sigma = 100$ .

(b) Following Lee and Kim,<sup>8</sup> the coefficients  $\{a_n, \dots, a_0, b_m, \dots, b_0\}$  are determined by the method of Pade approximation.<sup>12</sup> Briefly, the  $m + n + 1 = 2n$  coefficients are chosen so as to make the first  $2n$  terms of the Taylor series expansion of  $H_n^{n-1}(s)$  coincide with the first  $2n$  terms in the Taylor series of  $G(s)$ . For  $n = 1$ –3, the resulting approximants are given as follows:

$$H_1^0(s) = \frac{1}{\frac{1}{15}s + 1} \quad (9)$$

and

$$H_2^1(s) = \frac{\frac{2}{45}s + 1}{\frac{1}{945}s^2 + \frac{1}{9}s + 1} \quad (10)$$

and

$$H_3^2(s) = \frac{\frac{3}{5005}s^2 + \frac{4}{65}s + 1}{\frac{1}{135135}s^3 + \frac{2}{715}s^2 + \frac{5}{39}s + 1} \quad (11)$$

It is not hard to see that the models given by eqs 9–11 satisfy Properties 1 and 2. On the other hand, the fact that these approximants are PR transfer functions can be shown from a direct computation of  $\text{Re}[H_n^{n-1}(\sigma + j\omega)]$  by using the Maple computational package. For instance,

$$\operatorname{Re}[H_2^1(\sigma + j\omega)] = 21[(2\sigma^3 + 2\omega^2\sigma + 255\sigma^2 + 6615\sigma + 165\omega^2 + 42525)/(\sigma^4 + 2\sigma^2\omega^2 + 210\sigma^3 + 12915\omega^2 + \omega^4 + 210\omega^2\sigma + 9135\omega^2 + 198450\sigma + 893025)]$$

which is positive for all  $\sigma > 0$  and  $\omega \geq 0$ . Similar computations can be made for  $H_1^0(s)$  and  $H_3^2(s)$ . Further illustrations of the PR property of the approximants are given in Figure 2 where it is observed that  $\operatorname{Re}[H_n^{n-1}(\sigma + j\omega)] > 0$  for different values of  $\sigma > 0$ .

(c) Notice that the first-order approximant  $H_1^0(s) = 1/(1/15s + 1)$  is the classical LDF model proposed by Glueckauf.<sup>5</sup> In this way, a model of the form  $H_n^{n-1}(s)$  can be seen as a *generalized* LDF model for adsorption–diffusion processes. In fact, as  $a_0 = b_0 = 1$  can be chosen without losing generality, a state-space (i.e., time-domain) realization of the transfer function

$$H_n^{n-1}(s) = \frac{b_{n-1}s^{n-1} + b_{n-2}s^{n-2} + \dots + b_1s + 1}{a_ns^n + a_{n-1}s^{n-1} + \dots + a_1s + 1}$$

can be written as an  $n$ -dimensional linear differential system of the following form:<sup>9</sup>

$$\begin{aligned} \frac{dz}{d\tau} &= \mathbf{A}\mathbf{z} - \mathbf{B}(f(\tau) - \langle q \rangle) \\ \langle q \rangle &= z_1 \end{aligned} \quad (12)$$

where  $\mathbf{z} \in \mathbb{R}^n$  and the matrices  $\mathbf{A} \in \mathbb{R}^{n \times n}$  and  $\mathbf{B} \in \mathbb{R}^n$  are

$$\mathbf{A} \equiv \begin{bmatrix} -\alpha_{n-1} & 1 & 0 & \dots & 0 \\ -\alpha_{n-2} & 0 & 1 & \dots & 0 \\ \vdots & \vdots & \vdots & \ddots & \vdots \\ -\alpha_1 & 0 & 0 & \dots & 1 \\ -\alpha_0 & 0 & 0 & \dots & 0 \end{bmatrix}$$

and

$$\mathbf{B} \equiv \begin{bmatrix} \beta_{n-1} \\ \beta_{n-2} \\ \vdots \\ \beta_1 \\ \beta_0 \end{bmatrix}$$

where  $\alpha_i = (a_i - b_i)/a_n$  and  $\beta_i = b_i/a_n$ ,  $i = 0, \dots, n-1$ . Similar to the classical Glueckauf's LDF model given by eq 5, the dynamics of the state  $\mathbf{z}$  are driven by the "linear force"  $f(\tau) - \langle q \rangle$ . In this way, the approximant  $H_n^{n-1}(s)$  defines a generalized LDF model for adsorption–diffusion processes.

(d) In principle, by increasing the order of the approximant  $H_n^{n-1}(s)$ , it is possible to obtain better descriptions of the adsorption–diffusion dynamics. Figure 3 shows the Bode plots of  $G(s)$  and  $H_n^{n-1}(s)$ ,  $n = 1-3$ , where it is observed that, as  $n$  is increased, the frequency-response of  $G(s)$  is better approximated by the rational model  $H_n^{n-1}(s)$ . In fact, as the order is increased,  $H_n^{n-1}(s)$  obtains a closer fit of the high-frequency components of  $G(s)$ . This guarantees that the time-domain prediction of the average particle concentration is enhanced as higher-order approximants are used.

(e) Figure 3 shows that the rational functions  $H_n^{n-1}(s)$  have a good approximation of the frequency response

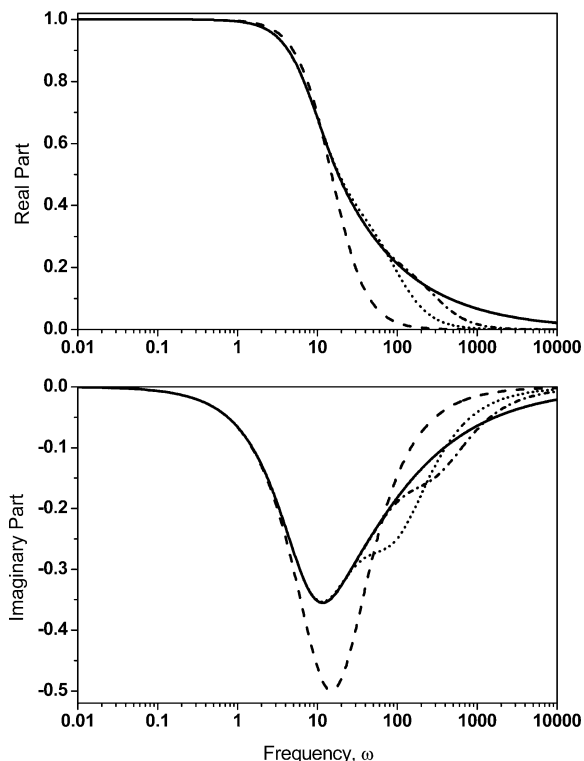


**Figure 3.** Bode plots of  $G(s)$  and  $H_n^{n-1}(s)$ ,  $n = 1-3$ , where it is observed that, as  $n$  is increased, the frequency-response of  $G(s)$  is better approximated by the rational model  $H_n^{n-1}(s)$ : —  $G(s)$ ; ---  $H_1^0(s)$ ; ...  $H_2^1(s)$ ; - · - ·  $H_3^2(s)$ .

$G(j\omega)$  into a limited frequency range  $[0, \omega_c(n)]$ . As discussed in the above paragraph, the upper limit  $\omega_c(n)$  increases as  $n$  increases. From Figure 3, one observes that  $\omega_c(1) \approx 3$ ,  $\omega_c(2) \approx 30$ , and  $\omega_c(3) \approx 90$ . For the noncyclic case where  $f(\tau) = f^*$ , the approximants  $H_n^{n-1}(s)$ ,  $n = 1-3$ , yield an accurate description of the adsorption phenomena around steady-state operating conditions. This explains the fact that the classical Glueckauf's LDF model works for most noncyclic operating conditions.<sup>1</sup> However, approximate rational models offer a limited description of cyclic adsorption dynamics. In particular, it has been shown that Glueckauf's LDF model (see eq 5) displays significant departures from the FD model  $G(s)$  for a wide range of practical cycling frequencies. This is because, out of the range  $[0, \omega_c(n)]$ , the adsorption dynamics description by  $H_n^{n-1}(s)$  is very poor. In the time domain, such departure of  $H_n^{n-1}(j\omega)$  from  $G(j\omega)$  is reflected as a large error in the average concentration trajectories.<sup>7</sup> As the limit frequency  $\omega_c(n)$  is an increasing function of  $n$ , the results in Figure 3 show that a more accurate description of the cyclic adsorption dynamics can be obtained when the approximation order is increased. In particular, the range of the operating frequencies that can be described by the second-order approximant  $H_2^1(s)$  is increased about 10 times. Such an increment in the approximation accuracy is made without an excessive increment in the complexity of the approximation model. In fact, the second-order model  $H_2^1(s)$  is still quite simple from the computational viewpoint since its solution involves only two linear ordinary differential equations. If refined computer simulations are required, a third-order model still has a simple structure,<sup>8</sup> involving only the implementation of three differential equations. A third-order model should suffice for simulating most practical

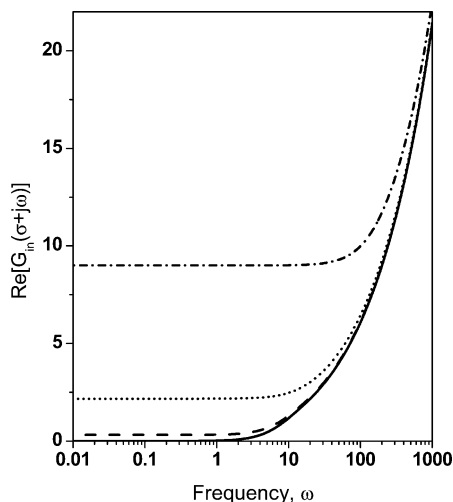


**Figure 4.** Real part of the complex function  $G_{in}(\sigma+j\omega)$  for different values of  $\sigma \geq 0$ . It is noticed that  $Re[G(\sigma+j\omega)] > 0$  for all  $\omega \in \mathbb{R}$  along four decades: —  $\sigma = 0$ ; ---  $\sigma = 1$ ; ...  $\sigma = 10$ ; - · - ·  $\sigma = 100$ .

situations as the cutting-off frequency  $\omega_c(3)$  is about 90 times the diffusion characteristic frequency  $\omega_D = 1/\tau_D$ . In fact, operating conditions for cyclic conditions use cycling frequencies  $\sim 2$ –5 times the characteristic frequency.<sup>1</sup>

(f) In practical cases, the average concentration  $\langle q \rangle$  is rarely the required response variable for equipment design and optimization. Indeed, the interfacial mass flux  $j_{in}$  is one important variable that should be monitored in order to assess the performance of the adsorption process. For the adsorption model given by eqs 1–3, the (dimensionless) interfacial mass flux is given by

$$j_{in}(\tau) = \frac{\partial q(\xi, \tau)}{\partial \xi} \Big|_{\xi=1}$$

It is not hard to show that  $J_{in}(s) = G_{in}(s)F(s)$ , where the transfer function  $G_{in}(s)$  is expressed as follows:

$$\begin{aligned} G_{in}(s) &= \frac{1}{3}sG(s) \\ &= s \left( \frac{\coth \sqrt{s}}{\sqrt{s}} - \frac{1}{s} \right) \end{aligned}$$

The function  $G_{in}(s)$  has the following properties: (1)  $\lim_{s \rightarrow 0} G_{in}(s) = 0$ , which means that  $j_{in} = 0$  at steady-state conditions (i.e., when  $f(\tau) = f^*$ ). (2)  $\lim_{s \rightarrow \infty} G_{in}(s) = \infty$ . This property says that high-frequency components of the forcing function  $f(\tau)$  are arbitrarily amplified when filtered by the transfer function  $G_{in}(s)$ . Contrary to the transfer function  $G(s)$ ,  $G_{in}(s)$  displays the structure of an unbounded high-pass filter where low-frequency disturbances are damped while high-frequency ones are unboundedly amplified. (3)  $G_{in}(s)$  is a PR function. In fact, Figure 4 shows that  $Re[G_{in}(s)] > 0$  for all  $\sigma > 0$ . That  $G_{in}(s)$  can be seen in advance since  $3((\coth \sqrt{s})/\sqrt{s} - 1/s)$  is PR (as shown above) and the operator  $s$  is also PR. In this form, the transfer function  $G_{in}(s)$  becomes PR. Similar to the approximants for the transfer function  $G(s)$ , approximants for  $G_{in}(s)$  should retain the properties described above. Property 1 indicates that  $H_{in,n}^m(s)$  should have a zero in the origin such that  $H_{in,n}^m(0) = 0$ . Since Property 2 implies unbounded frequency-response for high frequencies, it cannot be physically realized with causal (i.e.,  $m \leq n$ ) rational

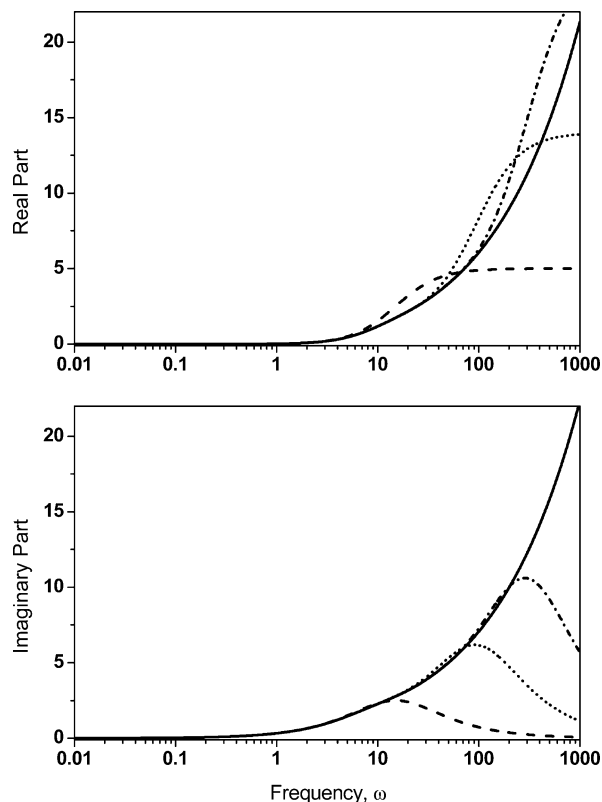


**Figure 5.** Bode plots of  $G_{in}(s)$  and  $sH_n^{n-1}(s)$ ,  $n = 1$ –3, where it is observed that, as  $n$  is increased, the frequency-response of  $G_{in}(s)$  is better approximated by the rational model  $sH_n^{n-1}(s)$ : —  $G_{in}(s)$ ; ---  $H_{in,1}^0(s)$ ; ...  $H_{in,2}^1(s)$ ; - · - ·  $H_{in,3}^2(s)$ .

transfer functions. In this way, physical considerations constrain the approximant class to satisfy  $m = n$ . Approximate rational models for  $G_{in}(s)$  can be easily obtained from the ones obtained for  $G(s)$ . In fact, one can exploit the fact that  $G_{in}(s) \equiv 1/3sG(s)$  and consider the approximation formulas  $H_{in,n}^n(s) \equiv 1/3sH_n^{n-1}(s)$ . Notice that, as  $H_n^{n-1}(0) = 1$ ,  $H_{in,n}^n(0) = 0$ , as required. However, the property  $\lim_{s \rightarrow \infty} G_{in}(s) = \infty$  cannot be met with a rational approximant  $H_{in,n}^n(s)$ . In fact, one should have  $\lim_{s \rightarrow \infty} H_{in,n}^n(s) = \gamma(n) < \infty$ . If  $H_{in,n}^n(s)$  is a uniform approximant, one can expect that  $\lim_{s \rightarrow \infty} \gamma(n) = \infty$ . This is shown in Figure 5 where it is observed that the goodness of the approximation  $H_{in,n}^n(s)$  increases as the order  $n$  is increased. It is also observed that the PR property of  $G_{in}(s)$  is retained by the approximants  $H_{in,n}^n(s)$ .

(g) An implementation of the approximant  $H_{in,n}^n(s)$  in the time domain can be made as a set of  $n$  linear differential equations. To do this, one can take advantage of the fact that, as showed in the above item,  $J_{in}(s) = (s/3)\langle Q \rangle(s)$ . In the time domain, one has<sup>9</sup>

$$j_{in}(\tau) = \frac{1}{3} \frac{d\langle q \rangle(\tau)}{d\tau} \quad (13)$$

That is, the interfacial mass flux  $j_{in}(\tau)$  is one-third the time-derivative of the average concentration  $\langle q \rangle$ . The approximate average concentration dynamics  $\langle q \rangle(\tau)$  can be obtained from a time-domain implementation of the approximant  $H_n^{n-1}(s)$ , as was shown in eq 12. Once  $\langle q \rangle(\tau)$  is obtained in such a form,  $j_{in}(\tau)$  is computed as in eq 13. A straightforward approach for computer simulation

is to use the backward finite-difference approximation

$$j_{\text{in}}(\tau) \approx \frac{1}{3} \frac{\langle q \rangle(\tau) - \langle q \rangle(\tau - \Delta\tau)}{\Delta\tau} \quad (14)$$

In this way,  $j_{\text{in}}(\tau)$  is computed from simultaneous implementations of the set of  $n$  linear differential equations (eq 12) and the time-derivative approximation (eq 14). A more systematic approach that is in accord with the passivity properties of the adsorption dynamics is to use a PR approximation of the time-derivative operator  $s$  as follows<sup>9</sup>

$$J_{\text{in}}(s) \approx \frac{s}{3(\tau_f s + 1)} \langle Q \rangle(s) \quad (15)$$

where  $\tau_f > 0$  is a filtering time constant. Notice that the exact time-derivative operator is recovered as  $\tau_f \rightarrow 0$ . The approximant (eq 15) can be described in a differential equation form as follows:

$$\begin{aligned} \frac{dW}{d\tau} &= -\frac{(\langle q \rangle + W)}{\tau_f} \\ j_{\text{in}} &= \frac{W + \langle q \rangle}{3\tau_f} \end{aligned} \quad (16)$$

That is, the Laplace transform of eq 16 is eq 15. The filtering time constant  $\tau_f$  plays a role similar to the step  $\Delta\tau$ . For practical implementation,  $\tau_f$  should be chosen to be sufficiently small. A heuristic rule is to choose  $\tau_f \sim 0.1$  times the diffusion time constant  $\tau_D = ((\epsilon_p + K) R_p^2)/D_p$ , which guarantees that only high-frequency components are washed out from the average concentration dynamics. Summing up, a computer implementation for simulation purposes would involve  $n + 1$  linear differential equations; namely,  $n$  differential equations to obtain  $\langle q \rangle(\tau)$  (see eq 12) and one differential equation to compute  $j_{\text{in}}(\tau)$  (see eq 16). The initial condition for all differential equations can be set to zero.

## 5. Conclusions

Because adsorption–diffusion models are derived from First Principles (i.e., mass balances), they contain the main physical dynamic characteristics of the phenomena. Thermodynamic features, such as irreversibility, are reflected in the structure of the model solutions. We have shown that positive realness (PR) properties are suitable algebraic tests to demonstrate the physical consistency of approximate dynamic models for adsorption processes. In fact, since PR refers to passivity, and this in turn relates to irreversibility, an approximate dynamic model for an adsorption–diffusion process should inherit this minimal structure. The result is a class of finite-dimensional (i.e., rational function) approximants that, for the average concentration dynamics, have the structure of generalized linear-driving force models. In this form, it was shown that a small increment in the approximation order can lead to a significant increment in the approximation accuracy.

## Appendix. Proof of Condition (iii) for $G(s)$ to Be PR

The proof is made by computing  $\text{Re}[F(\sigma + j\omega)]$ . With the aid of the Maple computational package, it can be

shown that

$$\text{Re}[F(\sigma + j\omega)] = \frac{1}{\chi(\sigma, \omega)} [\phi_1(\sigma, \omega) + \phi_2(\sigma, \omega) + \phi_3(\sigma, \omega) + \phi_4(\sigma, \omega)]$$

where

$$\begin{aligned} \chi(\sigma, \omega) &\equiv \\ &2\sqrt{(\sigma^2 + \omega^2)^3} \left[ -\cosh^2 \left( \frac{1}{2} \sqrt{(2\sqrt{\sigma^2 + \omega^2} + 2\sigma)} \right) \right] + \\ &\cos^2 \left[ \frac{1}{2} (\text{csgn}(\omega - j\sigma)) \sqrt{(2\sqrt{\sigma^2 + \omega^2} - 2\sigma)} \right] \end{aligned}$$

and

$$\begin{aligned} \phi_1(\sigma, \omega) &\equiv - \left[ \sinh \left( \frac{1}{2} \sqrt{(2\sqrt{\sigma^2 + \omega^2} + 2\sigma)} \right) \cosh \right. \\ &\left. \left( \frac{1}{2} \sqrt{(2\sqrt{\sigma^2 + \omega^2} + 2\sigma)} \right) \right] \sqrt{(2\sqrt{\sigma^2 + \omega^2} + 2\sigma)\sigma^2} \end{aligned}$$

and

$$\begin{aligned} \phi_2(\sigma, \omega) &\equiv - \left[ \sinh \left( \frac{1}{2} \sqrt{(2\sqrt{\sigma^2 + \omega^2} + 2\sigma)} \right) \cosh \right. \\ &\left. \left( \frac{1}{2} \sqrt{(2\sqrt{\sigma^2 + \omega^2} + 2\sigma)} \right) \right] \sqrt{(2\sqrt{\sigma^2 + \omega^2} + 2\sigma)\omega^2} \end{aligned}$$

and

$$\begin{aligned} \phi_3(\sigma, \omega) &\equiv \left\{ \sin \left[ \frac{1}{2} (\text{csgn}(\omega - \right. \right. \\ &j\sigma) \sqrt{(2\sqrt{\sigma^2 + \omega^2} - 2\sigma)} \right] \cos \left[ \frac{1}{2} (\text{csgn}(\omega - \right. \\ &j\sigma) \sqrt{(2\sqrt{\sigma^2 + \omega^2} - 2\sigma)} \right] \left\} (\text{csgn}(\omega - \right. \\ &j\sigma) \sqrt{(2\sqrt{\sigma^2 + \omega^2} - 2\sigma)\sigma^2} \end{aligned}$$

and

$$\begin{aligned} \phi_4(\sigma, \omega) &\equiv 2\sigma\sqrt{\sigma^2 + \omega^2} \left\{ \cosh^2 \left( \frac{1}{2} \sqrt{(2\sqrt{\sigma^2 + \omega^2} + 2\sigma)} \right) - \right. \\ &\left. \cos^2 \left[ \frac{1}{2} (\text{csgn}(\omega - j\sigma)) \sqrt{(2\sqrt{\sigma^2 + \omega^2} - 2\sigma)} \right] \right\} \end{aligned}$$

In the above equations, the following complex sign function has been used:

$$\text{csgn}(\omega - j\sigma) = \begin{cases} +1 & \text{if } \omega > 0 \\ -1 & \text{if } \omega \leq 0 \end{cases}$$

We will show that  $\text{Re}[F(\sigma + j\omega)] \geq 0$  for all  $\text{Re}[s] > 0$ . First, let us focus on the denominator  $\chi(\sigma, \omega)$ . Observe that  $(\sqrt{\sigma^2 + \omega^2})^3 > 0$  for all  $\text{Re}[s] > 0$ . On the other hand, we know that

$$\cos^2 \left[ \frac{1}{2} (\text{csgn}(\omega - j\sigma)) \sqrt{(2\sqrt{\sigma^2 + \omega^2} - 2\sigma)} \right] \leq 1$$

and

$$\cosh^2 \left( \frac{1}{2} \sqrt{(2\sqrt{\sigma^2 + \omega^2} + 2\sigma)} \right) > 1$$



for all  $Re[s] > 0$ . These inequalities imply that  $\chi(\sigma, \omega) < 0$  for all  $Re[s] = \sigma > 0$ . The numerator analysis will be carried out by parts. Observe that

1. Since  $\sinh(1/2\sqrt{(2\sqrt{\sigma^2 + \omega^2} + 2\sigma)}) > 0$  for all  $\sigma > 0$ , one determines that  $\phi_1(\sigma, \omega) < 0$  for all  $Re[s] > 0$ .

2. Similar to  $\phi_1(\sigma, \omega)$ ,  $\sinh(1/2\sqrt{(2\sqrt{\sigma^2 + \omega^2} + 2\sigma)}) > 0$  implies that  $\phi_2(\sigma, \omega) < 0$  for all  $Re[s] > 0$ .

3. To analyze  $\phi_3(\sigma, \omega)$ , consider the change of variable  $z(\sigma, \omega) \triangleq (\text{csgn}(\omega - j\sigma))\sqrt{(2\sqrt{\sigma^2 + \omega^2} - 2\sigma)}$ . Then, the following inequalities can be shown:

$$\begin{aligned} \sigma^2 z(\sigma, \omega) \sin\left(\frac{1}{2}z(\sigma, \omega)\right) \cos\left(\frac{1}{2}z(\sigma, \omega)\right) &= \sigma^2 z(\sigma, \omega) \sin z(\sigma, \omega) \\ &\leq \sigma^2 \sqrt{(2\sqrt{\sigma^2 + \omega^2} - 2\sigma)} \\ &\leq 0 \end{aligned}$$

for all  $Re[s] > 0$ . Consequently,  $\phi_3(\sigma, \omega) < 0$  for all  $Re[s] > 0$ .

4. Notice that  $\cosh^2(1/2\sqrt{(2\sqrt{\sigma^2 + \omega^2} + 2\sigma)}) > 1$  for  $\sigma > 0$ , and

$$\cos^2\left[\frac{1}{2}(\text{csgn}(\omega - j\sigma))\sqrt{(2\sqrt{\sigma^2 + \omega^2} - 2\sigma)}\right] \leq 1$$

In this way, similar to the case of the analysis of the denominator  $\chi(\sigma, \omega)$ , one concludes that  $\phi_4(\sigma, \omega) < 0$  for all  $Re[s] > 0$ .

The above analysis leads to the result that the sum  $\phi_1(\sigma, \omega) + \phi_2(\sigma, \omega) + \phi_3(\sigma, \omega) + \phi_4(\sigma, \omega) < 0$  for all  $\sigma > 0$ . As  $\chi(\sigma, \omega) < 0$  for all  $\sigma > 0$ , one concludes that  $Re[F(\sigma + j\omega)] > 0$  for all  $\sigma > 0$ . This concludes the proof.

## Nomenclature

$a_j$  = coefficients of the approximating polynomial  $A_n(s)$ ,  $0 \leq j \leq n$   
 $A_n(s)$  = approximating  $n$ -order polynomial in the denominator of  $H_n^m(s)$   
 $b_i$  = coefficients of the approximating polynomial  $B_m(s)$ ,  $0 \leq i \leq m$   
 $B_m(s)$  = approximating  $m$ -order polynomial in the numerator of  $H_n^m(s)$   
 $c$  = concentration in the particle, mol/m<sup>3</sup>  
 $c^*$  = characteristic concentration in the particle, mol/m<sup>3</sup>  
 $D_p$  = effective pore diffusivity, m<sup>2</sup>/sec  
 $f(\tau)$  = design parameter in the time domain  
 $F(s)$  = design parameter in the Laplace domain  
 $G(s)$  = transfer function relating  $\langle Q \rangle$  and  $F(s)$   
 $G_{in}(s)$  = transfer function relating  $J_{in}(s)$  and  $F(s)$   
 $H_n^m(s)$  = approximation of the transfer function  $G(s)$  by means of a polynomial of  $m$ -order in the numerator and  $n$ -order in the denominator  
 $H_{in,n}^m(s)$  = approximation of the transfer function  $G_{in}(s)$

$J_{in}(\tau)$  = dimensionless interfacial mass flux in the time domain

$J_{in}(s)$  = dimensionless interfacial mass flux in the Laplace domain

$k$  = constant in the Glueckauf model,  $k = 15$

$K$  = equilibrium constant

$q$  = dimensionless concentration per unit volume in the particle

$\langle q \rangle$  = average particle concentration, as defined in eq 4, in the time domain

$\langle Q \rangle$  = average particle concentration in the Laplace domain

$r$  = radial coordinate, m

$R_p$  = particle radius, m

$s$  = Laplace domain variable

$t$  = time, sec

$x$  = dimensionless radial position

## Greek Symbols

$\epsilon_p$  = porosity in the particle

$\tau$  = dimensionless time variable

$\tau_D$  = dimensionless diffusion time constant

$\tau_f$  = filtering time constant in eq 15

$\xi$  = dimensionless radial coordinate

## Literature Cited

- (1) Sircar, S.; Hufton, J. R. Why does linear driving force model for adsorption kinetics work? *Adsorption* **2000**, *6*, 137.
- (2) Zahed, A. H.; Epstein, N. Batch and continuous spouted bed drying of cereal grains: The thermal equilibrium model. *Can. J. Chem. Eng.* **1992**, *70*, 945.
- (3) Glueckauf, E.; Coates, J. Theory of chromatography. Part 4. The influence of effectiveness separation. *J. Chem. Soc.* **1947**, 1315.
- (4) Glueckauf, E. *Chem. Ind. (London)* **1955**, *34*, 187.
- (5) Glueckauf, E. Theory of chromatography. Part 10. Formulae for diffusion into spheres and their application to chromatography. *Trans. Faraday Soc.* **1955**, *51*, 1540.
- (6) Liaw, C. H.; Wang, J. S. P.; Greenkorn, R. A.; Chao, K. C. Kinetics of fixed-bed adsorption: A new solution. *AIChE J.* **1979**, *25*, 376.
- (7) Sheng, P.; Costa, C. A. V. Modified linear driving force approximations for cyclic adsorption-desorption processes. *Chem. Eng. Sci.* **1997**, *52*, 1492.
- (8) Lee, J.; Kim, D. H. High-order approximations for noncyclic and cyclic adsorption in a particle. *Chem. Eng. Sci.* **1998**, *53*, 1211.
- (9) Chen, C. T. *Introduction to Linear System Theory*; Holt Rinehart and Winston, Inc.: New York, 1970.
- (10) Narendra, K. S.; Taylor, J. H. *Frequency Domain Criteria for Absolute Stability*; Academic Press: New York, 1973.
- (11) Ydstie, B. E.; Alonso, A. A. Process systems and passivity via the Clausius-Planck inequality. *Syst. Control Lett.* **1997**, *30*, 253.
- (12) Bender, C. M.; Orszag, S. A. *Advanced Mathematical Methods for Scientists and Engineers*; McGraw-Hill: New York, 1978.

Received for review March 9, 2005

Revised manuscript received April 22, 2005

Accepted May 25, 2005

IE050329Z